International Journal of Hydrogen Energy 83 (2024) 1243–1250

Contents lists available at ScienceDirect

International Journal of Hydrogen Energy

journal homepage: www.elsevier.com/locate/he

Comparing the safety of bunkering LH_2 and LNG using quantitative risk assessment with a focus on ignition hazards

Jorgen Depken *, Maximilian Simon-Schultz, Lars Baetcke, Sören Ehlers

Institute of Maritime Energy Systems, German Aerospace Center (DLR), Dünebergerstraße 108, Geesthacht, 21502, Schleswig-Holstein, Germany

ARTICLE INFO

Keywords:
Safety
Bunkering
Hydrogen
QRA
Shipping
LNG

ABSTRACT

Liquid hydrogen represents a potential candidate for a climate neutral fuel for shipping. The utilization of this fuel necessitates the implementation of safe and reliable bunkering operations. This paper employs a quantitative risk assessment to compare the safety of bunkering liquid hydrogen with the safety of bunkering LNG. Initially, a frequency analysis is conducted using an event tree. It can be demonstrated, that the occurrence of the hazardous events, pool fire, flash fire and explosion, is more frequent with liquid hydrogen than with LNG. In the second step, the consequence analysis determines necessary safety distances for the hazardous events under consideration. For the events of pool fire and explosion, LNG-bunkering requires higher safety distances. Liquid hydrogen-bunkering requires higher distances for flash fire event. Since the safety distances for flash fire events are largest, they define the distances for the system. However, the consequences of flash fire events are subject to greater uncertainties and require further investigation. Overall, hazardous events occur more often with liquid hydrogen-bunkering, but LNG-bunkering requires in two out of three cases larger safety distances.

1. Introduction

Shipping is responsible for approximately 3% of global CO_2 emissions [1]. To meet the decarbonization targets of the Paris Climate Agreement, alternative fuels are being introduced in the shipping industry. In addition to methanol and ammonia, hydrogen is an option, especially for smaller units and shorter distances [2]. This can be used in either compressed or cryogenic liquefied form, although liquefied hydrogen may be a more attractive option due to its higher density. This paper therefore focuses on liquid hydrogen.

One of the concerns that has been raised in the discussion about the use of hydrogen in shipping is safety [3]. Hydrogen is considered to be a particularly dangerous fuel due to its high reactivity, which is also characterized by the fact that hydrogen is flammable from 4–75 vol% in air [4]. Liquefied Natural Gas (LNG), which is also a cryogenically liquefied flammable gas, is already used safely and reliably as a marine fuel and transported as cargo. The flammability range of LNG is narrower, with limits of 5.3–15 vol% [5].

The bunkering process is rarely considered in the literature. A search for the terms "hydrogen AND bunkering" in the Scopus database returns 43 results, whereas searching the same database for the terms "hydrogen AND ship" returns 1,717 results. Duong et al. [6] have published a review on ship-to-ship LNG bunkering. Saborit et al. [7] analyzed offshore produced hydrogen, the transport of hydrogen to the port and subsequent bunkering as fuel for ships. Duong et al. [8] employed numerical analysis to compare the safety zones due to dispersion during LNG and ammonia ship-to-ship bunkering. Fan et al. [9] presented a literature review on risk analysis methodology for LNG bunkering simultaneous operations, which included simultaneously bunkering and cargo operations or having passengers onboard.

Even if bunkering is not often considered in the literature, it poses particular challenges in term of safety. The receiving ship has to be connected to the shore or to another ship by means of flexible pipes or loading arms. This connection must, for example, compensate for ship motion or tidal range during the bunkering process, which at cryogenic temperatures poses particular challenges for the materials, due to temperature-induced embrittlement and stresses. Another example are detachable connections, which are prone to leakage.

Since LNG is already safely used in shipping and is a comparable substance, its bunkering safety is evaluated in comparison to that of liquid hydrogen. A quantitative risk analysis (QRA) was chosen as the most objective method for comparing the bunkering of the two fuels.

Many risk analysis methods rely on "expert judgment". For example, in Failure Mode and Effect Analysis (FMEA) the severity, probability of occurrence and probability of detection of a failure are rated by a team using catalogs ranging from 1 to 10 [10]. Quantitative risk

* Corresponding author.
E-mail address: jorgen.depken@dlr.de (J. Depken).

https://doi.org/10.1016/j.ijhydene.2024.08.177
Received 9 April 2024; Received in revised form 15 July 2024; Accepted 10 August 2024

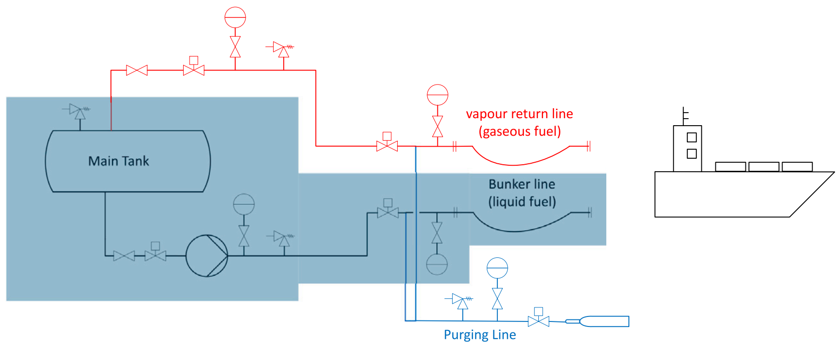

Fig. 1. Conceptual design of considered bunker system for LNG and LH_2, die scope of this paper is highlighted in blue. (For interpretation of the references to color in this figure legend, the reader is referred to the web version of this article.)

analysis, on the other hand, does not depend on the expert judgment. It uses an evaluation of data from existing systems to analyze the probability of failure and physical models to analyze the potential consequences [11].

Tofalos et al. [12] have previously conducted a quantitative risk analysis (QRA) to assess the safety of the ship-side bunker system, from the coupling in the bunker station to the receiving tank, for the two fuels under consideration. The use of a QRA for bunkering was previously established by Jeong et al. [13] who used the QRA to establish safety exclusion zones for LNG bunkering. In this work, the shoreside bunker system – from donating tank to bunker station – is now analyzed. For this purpose, some modifications are made to the methodology used by Tofalos et al. By combining the results of Tofalos et al. with those of this study a comparison of the complete bunker system, from tank to tank can be made.

2. Material and methods

This chapter first describes the use case. Based on this, the frequency analysis and the consequence analysis are presented.

2.1. Use case

To perform the QRA, it is necessary to define a ship and a bunker station as a use case. A small cruise ship with a length of about 140 m and an engine power of 11.2 MW is selected as the vessel for this analysis. A voyage time of 7 days is assumed, which results in a power demand of 4,516 MWh, assuming an energy efficiency of 0.5 and a fuel margin of 1.2. The fuel margin includes the fact that ships carry more fuel than necessary for the voyage to be able to respond to unforeseen events, such as heavy weather.

The bunker station is assumed to be a port-to-ship station at a cruise center. It is assumed that 280 bunkering operations will be performed by this station each year. This corresponds to the number of cruise ships calling the port of Hamburg in 2023 [14]. Not all ships may use hydrogen in the future, especially larger units, but this can be compensated by other ship types, such as dredgers, also using the bunker station. It is assumed that the pipe diameter of the bunker system will be 150 mm, resulting in a transfer rate of 22.5 t/h for liquid hydrogen and 289 t/h for LNG. This results in a duration of 6 h for liquid hydrogen and 1.2 h for LNG for a single bunkering operation.

The system used for the QRA is illustrated in Fig. 1. It should be noted that the system under consideration is not intended to be operational; rather, it is designed to serve as a basis for the risk assessment. The scope of this comparison is also limited to the liquid system, highlighted in blue in Fig. 1. The vapor return and purging systems are outside the scope of this paper. The equipment considered in this paper is shown in Table 1. In this table the diameter for the tank is not the actual tank diameter, but the diameter of the inlets.

2.2. Frequency analysis

The frequency analysis follows an event tree established by Jeong [15] and shown in Fig. 2. Outcome events of this event tree can be no accident, a pool fire (see chapter 2.3.1), a flash fire (see chapter 2.3.2) or an explosion (see chapter 2.3.3). The steps of the event tree are discussed further in the following subsections.

2.2.1. Initial leak

The occurrence of an unsafe situation is contingent upon the release of fluid through a leak. This leak is the initial step in the event tree and is described in the following chapter. For the purpose of this paper the leak frequencies established by the International Association of Oil & Gas Producers (IOGP) [16] are employed. To obtain the leak frequencies, the IOGP analyzed 4664 reported releases in the United Kingdom Health and Safety Executives hydrocarbon release database (HCRD). It considered 24 different equipment types and included the release frequency as a function of equipment size and leak diameter.

The results of the analysis are functions for the different equipment types as a function of equipment diameter and hole size. These functions have the form shown in Eq. (1), where the parameters C, m and B can be taken from a table as a function of equipment diameter and d is the hole diameter.

$$F(d) = C \cdot d^m + B \tag{1}$$

Although the data was obtained from the offshore industry, it can be used for other purposes. Its use for bunkering infrastructure was established by Tofalos et al. [12], who used failure frequencies from DNV [17], also based on the HCRD.

To obtain a system-wide leak frequency the frequency for an individual piece of equipment is calculated and then multiplied by the number of that equipment installed in the system. Once this has been done for all equipment, the individual values are added together and multiplied by the bunker frequency to obtain the failure frequency for the entire system.

2.2.2. Event tree

Following the initial release of fuel, Hydrogen or Natural Gas, subsequent events must occur, to cause harm to people. The probabilities of these events are considered by an event tree. Fig. 2 shows this event tree.

After the initial release, the fuel may ignite immediately, causing a pool or jet fire. Ignition probabilities are discussed in detail in chapter 2.2.3. If it ignites immediately, the branch of the event tree is already complete; if it does not ignite, further steps may lead to an unsafe situation.

It is assumed that the only safety mechanism is a watchkeeper on deck who can stop the bunkering process if he notices irregularities. In this paper it was assumed that the watchkeeper can usually react in a timely and appropriate manner, so that in 90 % of the cases the leak

Table 1
Equipment of bunkering system and leak frequencies as described in chapter 2.2.1.

Equipment	Diameter (mm)	Count	Single leak frequency per year			System leak frequency per year		
			3 mm	50 mm	150 mm	3 mm	50 mm	150 mm
Tank Inlet	150	1	3.15E−04	4.92E−05	2.38E−05	3.15E−04	4.92E−05	2.38E−05
Pressure Relieve Valve	150	2	6.31E−05	7.89E−06	3.60E−06	1.26E−04	1.58E−05	7.20E−06
Pressure Indicator	50	2	7.65E−05	6.62E−06		1.53E−04	1.32E−05	
Pipes	150	10	6.11E−06	5.39E−07	2.09E−07	6.11E−05	5.39E−06	2.09E−06
Hose	150	30	1.67E−04	4.77E−05	2.93E−05	5.01E−03	1.43E−03	8.78E−04
Actuated Valves	150	2	6.31E−05	7.89E−06	3.60E−06	1.26E−04	1.58E−05	7.20E−06
Manual Valves	150	3	1.35E−05	1.65E−06	7.27E−07	4.04E−05	4.95E−06	2.18E−06
Flanges	150	17	5.39E−06	8.77E−07	5.58E−07	9.16E−05	1.49E−05	9.48E−06
Pump (centrifugal)	150	1	7.94E−04	1.78E−05	4.04E−06	7.94E−04	1.78E−05	4.04E−06
Total Summation						6.72E−03	1.57E−03	9.34E−04
LH2 Inital Frequency with Bunker Duration						1.29E−03	3.01E−04	1.79E−04
LNG Inital Frequency with Bunker Duration						2.56E−04	5.97E−05	3.56E−05

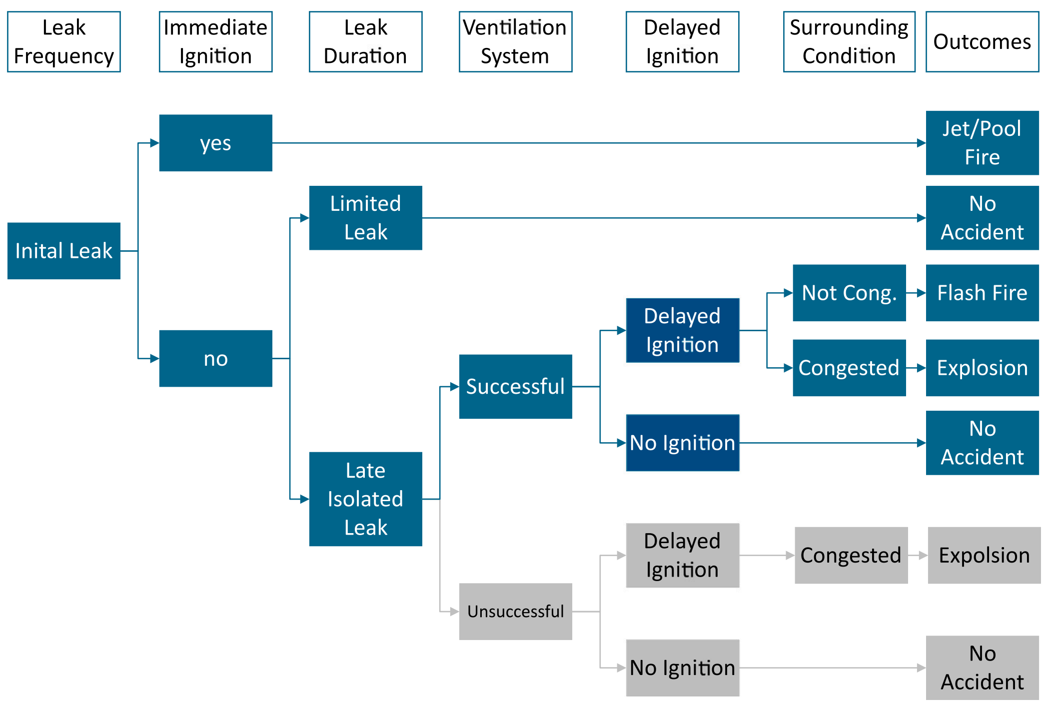

Fig. 2. Event tree used for frequency analysis [15].

was limited and no accident occurred. In 10 % of the cases, however, a late isolated leak occurred and an accident was still possible [12]. This assumption does not affect the comparison since it is the same for both fuels.

Bunkering usually takes place on open deck, so there was only natural ventilation and the ventilation system cannot fail. The result was a 100 % probability of successful ventilation and therefore the following branch of unsuccessful ventilation is grayed out in Fig. 2.

After the fuel was vaporized and dispersed, it could ignite again. The probability for this delayed ignition is also described in chapter 2.2.3. If it did not ignite, there was no accident. If it did ignite, a flash fire or explosion was possible, depending on the surrounding conditions. If the fuel vapor was trapped in a congested space, overpressure built up and the fuel burned by means of an explosion. If the gas was not in a congested space, a flash fire occurred that did not build up overpressure. Since bunkering is done on open deck, it was assumed that 20 % of the surrounding was congested, while 80 % was not [12]. Again, this assumption does not affect the comparison as it is the same for both fuels.

2.2.3. *Ignition probabilities*

Several models have been developed for the purpose of calculating ignition probabilities. Three have been considered for this work and are briefly described below.

Cox et al. [18] introduced a simple ignition probability model. The model distinguished only between gases and liquids and provided a curve for both states of aggregation from which the ignition probability could be read as a function of release rate. It did not distinguish between the reactivity of the substances. There was also no distinction between direct and delayed ignition. An approximation for the curve for gases was given by Eq. (2) [12]. Since the model is not particularly differentiated, it is not selected for this paper.

$$PR_I = 0.0158 * Q_L^{0.6145} \tag{2}$$

PR_I: ignition probability; Q_L: initial liquid release rate, in kg/s;

The model described in the Dutch Reference Manual Bevi Risk Assessments [19] was based on a simple table from which the probability of direct ignition could be calculated as a function of the leak rate and the reactivity of the substance. It was assumed that a released substance always ignites, which meant that the probability of a delayed ignition

Table 2
Ignition probabilities according to Energy Institute model.

Case No.	Case description	Release rate range (kg/s)	Equation
5	Small Plant Gas LPG	0.1–1	$P_{ign} = 0.00250 \cdot Q^{0.357}$
		1–3	$P_{ign} = 0.00250 \cdot Q^{1.568}$
		3–498	$P_{ign} = 0.00624 \cdot Q^{0.735}$
		> 498	$P_{ign} = 0.600$

Table 3
Specific heat input into a pool of cryogenic liquid [22].

Heat input by	Heat source q [kW/m²]	
	LH_2	LNG
Atmospheric convection	0.8	1.1
Radiation from flame	12	100-200
Radiation from ambient	1.6	1.6
Conduction from ground	100	9.2

was $1 - ProbabilityDirectIgnition$. Given the inherent conservatism of the approach that a released flammable gas always ignites, this model is also not considered further.

The UKOOA model, developed by the Energy Institute and described by the IOGP [20], employs 28 mathematical formulas derived from 28 environmental conditions to calculate the probability of ignition (direct + delayed). It was assumed that the probability of direct ignition was always 0.001, regardless of the environment or release rate. To calculate the probability of delayed ignition, the probability of direct ignition was subtracted from the total probability. According to the IOGP, this method was not applicable to LNG. The reason was that heat transfer and vaporization effects could have resulted in incorrect gas quantities. Nevertheless, it is used in this paper because it is too conservative if the values for a pure gas release are selected. For "very reactive substances" such as hydrogen, the probabilities were doubled. For this paper, the environmental conditions from Case 5 "Small Plant Gas LPG" are identified as being most appropriate for a bunkering station. The calculation of the ignition probability is described in Table 2.

The leak rate to be used in Table 2 is calculated according to Eq. (3) [17]. For this paper a height of 30 m and a liquid pressure of $5 \cdot 10^5$ N/m² is assumed.

$$Q_L = C_D \cdot A \cdot \sqrt{2 \cdot \rho_L[(P_0 - P_a) + \rho_L g h]} \tag{3}$$

Q_L: initial liquid release rate, in kg/s; C_D: discharge coefficient (= 0.61); A: hole area, in m²; ρ_L: liquid density, in kg/m³; P_0: initial absolute pressure of liquid, in N/m²; P_a: atmospheric pressure (= 10^5 N/m²); g: acceleration of gravity (= 9.81 m/s²); h: height of liquid surface above hole m

Since the UKOOA model has a good level of detail and can distinguish between direct and delayed ignition, it is used in this work.

2.3. Consequence analysis

After analyzing the frequency of the three hazardous events considered in this paper – pool fire, flash fire and explosion – the consequences of these events must be analyzed to determine safety distances.

2.3.1. Pool fire

The primary hazard to humans from a pool fire is the heat radiation emitted by the flame. In order to calculate the radiation emitted by the flame, it is first necessary to determine the size of the resulting pool and flame. The size of a cryogenic liquid pool is determined by the heat input into the pool and the heat of vaporization of the liquid. The heat input to the pool consists of heat conduction from the ground Q_{cond}, heat convection from the surroundings Q_{conv}, heat radiation from the surroundings Q_{long} and Q_{rad} [21], and possibly heat radiation from the flame Q_{flame}, see equation (4). Most models of a cryogenic pool did not take the flame into account. In this work, however, the proportion of the resulting heat input is so large that the flame is taken into account. Aside from the heat input of the flame, the largest heat source of the pool is the ground. However, as the ground cools from contact with the cold liquid, the pool will actually continue to expand as long as liquid is added and no fire is created.

$$Q_{Pool} = Q_{cond} + Q_{conv} + Q_{rad} + Q_{long} + Q_{flame} \tag{4}$$

Since the calculation of the individual components of the heat input is relatively complex, the values of Verfondern and Dienhart [22], which can be taken from Table 3, are used in this work.

The values derived above can be used to calculate the area A of the pool in the equilibrium state of inflow and evaporation, according to Eq. (5). Assuming circular spread, the diameter of the pool can also be calculated directly from the area.

$$A = \frac{Q_L \cdot \Delta H_V}{q_{cond} + q_{conv} + q_{rad} + q_{flame}} \tag{5}$$

A: area covered by the pool, in m²; Q_L: leak rate, in [kg/s]; ΔH_v heat of vaporization, in [kJ/kg]; q_{cond}, q_{conv}, q_{rad} and q_{flame} are variables from Eq. (4), normalized to the area, in [kW/m²];

It should be noted that a fraction of the emitted radiation is absorbed by the atmosphere, depending on the relative humidity. The transmissivity of the atmosphere τ_{atm} is calculated according to Eq. (6) [21].

$$\tau_{atm} = 1.5092 - 0.0708 \cdot ln\left(R_d \cdot P_{w,sat}(T_a) \cdot \frac{RH}{100}\right) \tag{6}$$

τ_{atm} transmissivity of the atmosphere, dimensionless; R_d is the distance traveled, in m; $P_{w,sat}(T_a)$ is the saturation vapor pressure of water, in Pa, see Eq. (7); T_a is the atmospheric temperature, in K; RH is the relative humidity, in %;

$$P_{w,sat} = exp(25.897 - 5319.4/T_a) \tag{7}$$

$P_{w,sat}(T_a)$ is the saturation vapor pressure of water, in Pa; T_a is the atmospheric temperature, in K;

With the transmissivity of the atmosphere, the radiation on an object Q_{rad} at a distance R_d is calculated using the point source model described in Eq. (8) [23].

$$Q_{rad}(R_d) = \tau_{atm} \cdot \chi_R \cdot \frac{(\pi/4) \cdot D^2 \cdot C_b \cdot \Delta H_C}{4 \cdot \pi \cdot R_d^2} \tag{8}$$

$Q_{rad}(R_d)$: radiation on an object at a distance R_d, in kW/m²; χ_R: fraction of combustion energy released, that is radiated (0.045 for LH_2 and 0.22 for LNG); D: Diameter of the fire, in m; $C_b = 10^{-3} \cdot \Delta H_c/\Delta H_v$ liquid mass combustion flow, in kg/m² s; ΔH_c lower heat of combustion, in kJ/kg; ΔH_v heat of vaporization, in kJ/kg.

2.3.2. Flash fire

A flash fire is defined as a combustion event in which a gas cloud ignites and burns without an increase in pressure. It can occur, when a combustible concentration of gas is present. The distance at which the gas has dispersed below the lower flammability limit is considered a safety distance in this case. To calculate this distance, a Gaussian dispersion model is used. These Gaussian models were designed for the simulation of pollutant in small concentrations, rather than for the prediction of flammable gas releases in high concentrations. Despite the limitations of these models, they are employed in this context due to the lack of more suitable alternatives in the literature and the extensive computational requirements of CFD analysis. A simplified version of this model, which considers only the downwind direction (x-direction) is presented in Eq. (9) [24].

$$C(x, 0, 0) = \frac{Q_L}{\pi u_w \sigma_y \sigma_z} \tag{9}$$

$C(x,0,0)$: Concentration at some point in space in kg/m^3; u_w: wind speed in m/s (here 5 m/s); σ_y and σ_z: dispersion constants as functions of the distance and the wind stability class, in m;

The parameters σ_y and σ_z can be obtained for the various wind stability classes from the relevant graphs. The wind stability was classified into six classes, ranging from A (least stable) to F (most stable). The classes depended on weather factors such as wind speed, solar radiation and cloud coverage [24]. As indicated by Jeong [15], Eqs. (10) and (11) were employed to approximate the aforementioned graphs. For the purposes of this study, the wind stability class F was selected, as it represents the most stable condition and allows for the least dispersion, thereby ensuring the highest safety distances.

$$\sigma_y = 0.04 \cdot R_d \cdot (1 + 0.0001 \cdot R_d)^{-0.5} \quad (10)$$

$$\sigma_z = 0.016 \cdot R_d \cdot (1 + 0.0003 \cdot R_d)^{-1} \quad (11)$$

Eq. (8) illustrates the concentration in kg/m^3. To convert this value into volume percent, the concentration is divided by the density of the gas and multiplied by 100, as shown in Eq. (12).

$$C_v(x,0,0) = \frac{C(x,0,0)}{\rho_g} \cdot 100 \quad (12)$$

$C_v(x,0,0)$: Concentration at some point in space in vol%; ρ_g: density of flammable gas, in kg/m^3;

2.3.3. Explosion

When a gas cloud ignites with an increase in pressure, this phenomenon is known as an explosion. In this case, the increase in pressure is the primary hazard for humans. The TNT Equivalency Explosion Model is employed to calculate the pressure increase resulting from the explosion. This model is relatively straightforward, yet its accuracy is limited. If the environmental conditions are known with greater precision, other models, such as the TNO model or the Baker–Strehlow–Tang model, are preferable [21]. However, as this information is not available for this comparison, the TNT Equivalency Explosion Model is employed.

To determine the overpressure caused by an explosion, the equivalent mass of TNT was initially calculated from the available quantity of gas using equation (13) [25].

$$W_{TNT} = \frac{m_v \cdot \eta \cdot \Delta H_{c(gas)}}{\Delta H_{c(TNT)}} \quad (13)$$

W_{TNT}: equivalent mass of TNT, in kg; m_v: total mass of flammable gas, in kg; η: explosion yield, dimensionless (= 0.1); $\Delta H_{c(gas)}$: lower heat of combustion of gas, in kJ/kg; $\Delta H_{c(TNT)}$: lower heat of combustion of TNT (= 4680 kJ/kg);

With the equivalent mass the scaled distance was calculated according to Eq. (14) [25].

$$Z = \frac{R_d}{W_{TNT}^{1/3}} \quad (14)$$

Z: scaled distance, in $m/kg^{1/3}$;

Lobato et al. [25] presented a graph that was used to convert the scaled distance into the overpressure. Tofalos et al. [12] provided an approximation of this graph in Eq. (15).

$$P_S = 573 \cdot Z^{-1.685} \quad (15)$$

P_S: overpressure, in kPa;

3. Results

The results of the frequency and consequence analysis are presented below. Safety distances are then defined based on these results.

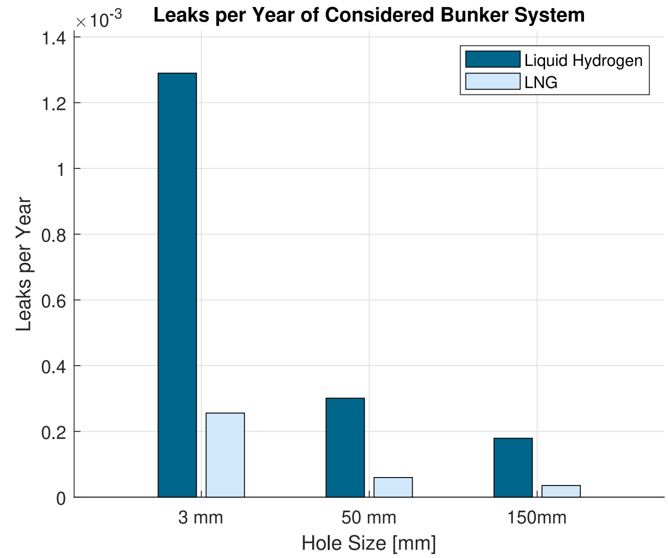

Fig. 3. Initial leaks per year.

3.1. Frequency analysis

The start of the event tree is the initial leak of LH_2 or LNG. The leakage rate for each type of equipment and hole size is calculated individually, as described in chapter 2.2.1, and can be found in Table 1. The leakage rate for each piece of equipment is multiplied by the number of times it is installed and all equipment types are added together. Finally, the different bunker durations of the two fuels are taken into account. These individual calculation steps can be seen in Table 1. The results are the initial leaks per year and are shown in Fig. 3. These values are incorporated into the subsequent calculations presented in Table 4.

In this study, three hole diameters are considered: 3, 50 and 150 mm. The 150 mm diameter represents a full rupture of the equipment. For all hole sizes, the frequency of liquid hydrogen leaks is five times higher than for LNG, although the frequencies for the equipment and the system itself are the same. The bunkering process of LNG takes approximately 1.2 h, whereas the same process for LH_2 takes 6 h. The longer duration results in the different occurrence of leaks for the fuels.

For instance, $1.29 \cdot 10^{-3}$ leaks per year for the 3 mm LH_2 leak implies, that a bunker system must operate for approximately 775 years or for 775 bunker systems to be operational for one year for a leak to statistically occur.

Table 4 presents the remaining steps of the event tree, as described in chapter 2.2. By multiplying the columns, the number of hazardous events per year can be calculated. These events can also be found in Fig. 4. The horizontal line in Fig. 4 represents a frequency of 10^{-6}, which is a broadly accepted individual risk per annum (IRPA) for members of public [11,26]. Fig. 4 illustrates that liquid hydrogen reaches the threshold of 10^{-6} in four cases, with a maximum of $4.58 \cdot 10^{-6}$ events per year. In contrast, LNG is consistently below this level.

This work does not consider social risk because it requires additional assumptions about the ship and its surroundings. For a specific system, social risks should also be considered.

3.2. Consequence analysis

In general, the consequences are the three hazardous events: pool fire, flash fire and explosion. The results of these events, for a pool fire, include heat radiation; for a flash fire, dispersion and for an explosion, overpressure. These results are calculated and presented in the following sections.

Table 4
Results of frequency analysis.

Fuel	Leak size	Initial leaks per year	Fire type	Immediate ignition	Leak duration	Ventilation system	Delayed ignition	Surrounding conditions	Ignition probability	Events per year
LNG	3 mm	2.56E−04	Pool Fire	0.001	–	–	–	–	1.00E−03	2.56E−07
			Flash Fire	0.999	0.1	1	0.0001	0.8	7.99E−06	2.04E−09
			Explosion	0.999	0.1	1	0.0001	0.2	2.00E−06	5.11E−10
	50 mm	5.97E−05	Pool Fire	0.001	–	–	–	–	1.00E−03	5.97E−08
			Flash Fire	0.999	0.1	1	0.0682	0.8	5.45E−03	3.26E−07
			Explosion	0.999	0.1	1	0.0682	0.2	1.36E−03	8.14E−08
	150 mm	3.56E−05	Pool Fire	0.001	–	–	–	–	1.00E−03	3.56E−08
			Flash Fire	0.999	0.1	1	0.3469	0.8	2.77E−02	9.86E−07
			Explosion	0.999	0.1	1	0.3469	0.2	6.93E−03	2.46E−07
LH_2	3 mm	1.29E−03	Pool Fire	0.002	–	–	–	–	2.00E−03	2.58E−06
			Flash Fire	0.998	0.1	1	0.0002	0.8	1.60E−05	2.06E−08
			Explosion	0.998	0.1	1	0.0002	0.2	3.99E−06	5.15E−09
	50 mm	3.01E−04	Pool Fire	0.002	–	–	–	–	2.00E−03	6.02E−07
			Flash Fire	0.998	0.1	1	0.0621	0.8	4.95E−03	1.49E−06
			Explosion	0.998	0.1	1	0.0621	0.2	1.24E−03	3.73E−07
	150 mm	1.79E−04	Pool Fire	0.002	–	–	–	–	2.00E−03	3.58E−07
			Flash Fire	0.998	0.1	1	0.3201	0.8	2.56E−02	4.58E−06
			Explosion	0.998	0.1	1	0.3201	0.2	6.39E−03	1.15E−06

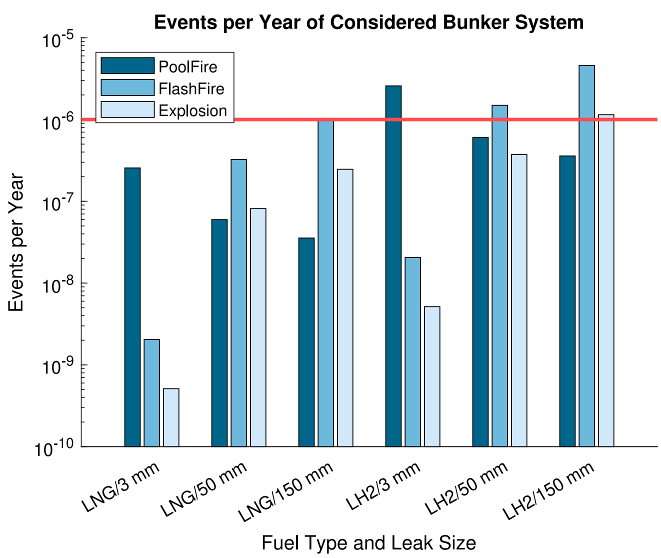

Fig. 4. Events per year, the horizontal line marks the IRPA of 10^{-6}.

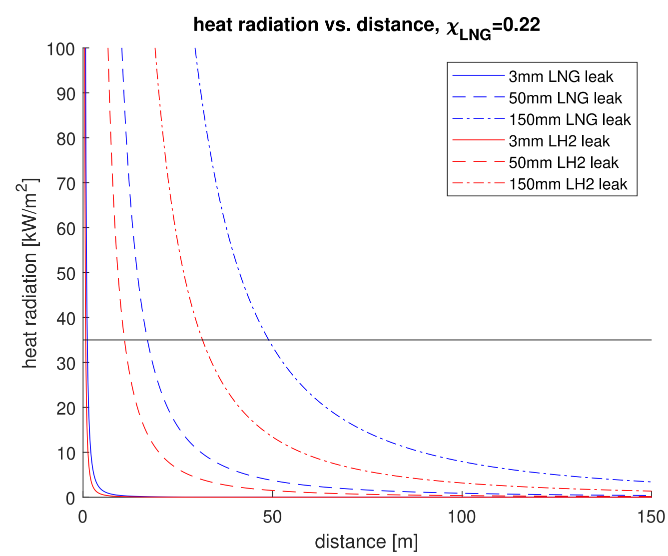

Fig. 5. Heat radiation caused by pool fire (the horizontal lines marks the lethal radiation of 35 kW/m²).

3.2.1. Pool fire

The heat radiation from a pool fire is calculated according to chapter 2.3.1 and the resulting values are presented in Fig. 5. The calculated pool diameters vary between 0.26 m for a 3 mm LH_2 leak and 36.98 m for the 150 mm LNG leak. The heat radiation at a distance of 50 m varies between 0.63 kW/m² for a 3 mm LH_2 leak and 36.98 kW/m² for the 150 mm LNG leak. In Fig. 5, the level of 35 kW/m², which is the level of significant probability of death [27], is marked with a horizontal line.

3.2.2. Flash fire

To calculate where a flash fire can occur, the dispersion of the fuels is calculated using a Gaussian model, described in chapter 2.3.2. The concentration of fuel in the wind direction can be seen in Fig. 6, where the lower flammability limits of hydrogen (4%) and LNG (5.3%) are marked as a horizontal line.

3.2.3. Explosion

For the purpose of calculating the safety distance of an explosion, an overpressure of 1 bar is assumed to be the level at which a certain death would occur [12]. In order to calculate the overpressure, the TNT equivalent model, as described in chapter 2.3.3, is used. The results can be found in Fig. 7. From which it can be observed that LNG has slightly

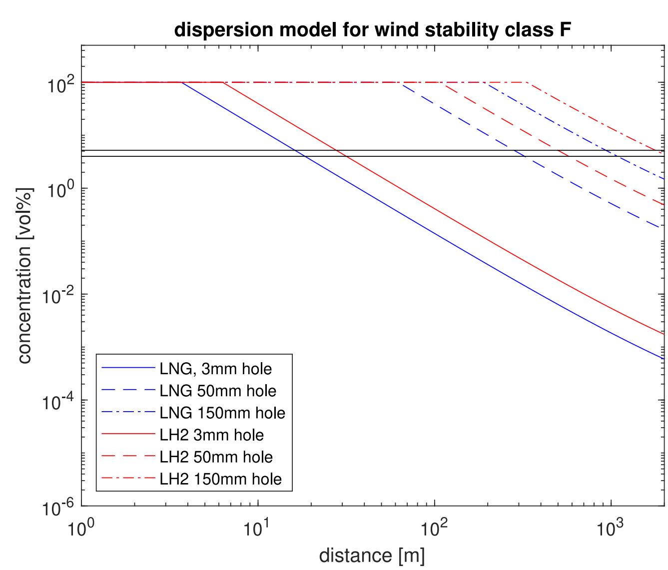

Fig. 6. Dispersion of hydrogen and LNG (the horizontal lines mark the lower flammability limits of H_2 and LNG).

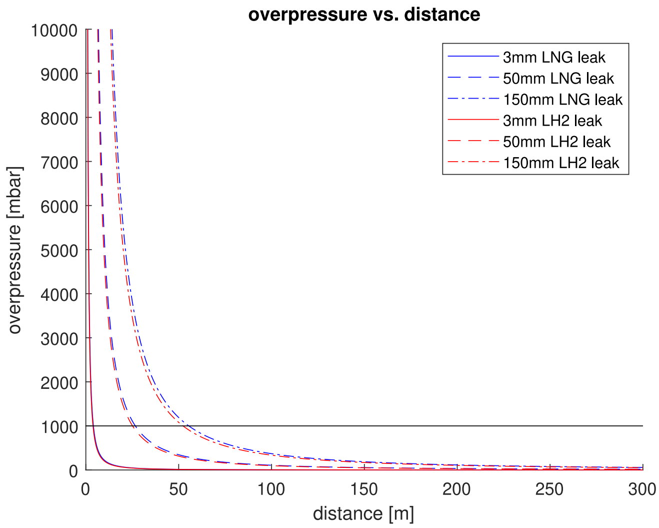

Fig. 7. Explosion overpressure vs distance (the horizontal lines marks the lethal overpressure of 1000 mbar).

Table 5
Safety distances from consequence analysis.

Fuel	Leak size (mm)	Safety distance (m) pool fire	vapor cloud explosion	flash fire
LNG	3	1.2	4.1	17
	50	17	26.7	279
	150	49	55.4	922
LH_2	3	0.8	3.9	32
	50	11	25.2	576
	150	32	52.3	2108

higher pressures than LH_2. At a distance of 50 m, an explosion resulting from a 50 mm LNG leak would result in an overpressure of 347 mbar, whereas the same leak with hydrogen would result in an overpressure of 314 mbar.

3.3. Defining safety distances

The preceding chapters have yielded data that can be used to calculate the distances at which the aforementioned limits are reached. This information can be found in Table 5. It can be observed, that LNG requires larger safety distances for pool fires and explosions, whereas LH_2 requires larger distances for a flash fire.

4. Discussion

The frequency analysis indicates that hydrogen is more likely to experience leaks. As the same system is utilized for this comparison, the equipment employed and its quantity have no impact on the probability of occurrence. Only the longer bunker duration due to the lower density of hydrogen and the higher ignition probabilities of hydrogen due to its higher reactivity have an effect.

The consequence analysis reveals that LNG necessitates greater safety distances for the explosion and pool fire. Only for the flash fire, hydrogen requires larger safety distances. Since LNG is below the limit of 10^{-6} for the individual risk per annum (IRPA) in all cases in the frequency analysis, it is generally not necessary to consider the safety distances of LNG. In contrast, the safety distances of the four cases that are above the limit in Fig. 4 must be considered for hydrogen. However, as the objective of this study is not to perform a quantitative risk assessment (QRA) for a specific application, but rather to compare the fuels liquid hydrogen and LNG, all safety distances are considered in this case.

The safety distances of LNG are higher than those of LH_2 for pool fires and for explosions. However, for flash fires, the safety distance is larger for LH_2 and is also the largest of all the cases considered.

The flash fire, or the dispersion of the fuels, is calculated using a simple Gaussian model. This model does not consider the buoyancy of a substance or the influence of the change in density as a substance heats up. LNG (methane) is eight times heavier than hydrogen and therefore has significantly less buoyancy [28]. Additionally, when hydrogen vaporizes, it only requires a 2 K increase in temperature to become lighter than air. In contrast, LNG requires a 53.3 K increase in temperature [5]. These factors are not accounted for in the model and should be investigated in more detail through a CFD analysis.

The largest safety distance of the cases considered defines the safety distance of the system. Therefore, a distance more than twice as large must be maintained during the bunkering of hydrogen than when LNG is bunkered. However, LNG is above hydrogen in all other cases.

5. Conclusions

Leaks at hydrogen plants occur more frequently and larger safety distances must also be maintained, whereby the safety distances should be validated again using CFD analyses.

Consequently, the bunkering of hydrogen can be considered more dangerous than the bunkering of LNG. Further research into the safety of hydrogen as a fuel for shipping is therefore necessary to facilitate the market launch of liquid hydrogen. An increase in demand for liquid hydrogen will facilitate the growth of the entire liquid hydrogen value chain. Furthermore, the research results will positively impact the import of liquid hydrogen, as the loading and unloading processes for ships are analogous to bunkering.

CRediT authorship contribution statement

Jorgen Depken: Writing – review & editing, Writing – original draft, Visualization, Project administration, Methodology, Investigation, Formal analysis, Conceptualization. **Maximilian Simon-Schultz:** Writing – review & editing, Writing – original draft, Methodology, Investigation. **Lars Baetcke:** Supervision. **Sören Ehlers:** Supervision.

Declaration of competing interest

The authors declare that they have no known competing financial interests or personal relationships that could have appeared to influence the work reported in this paper.

Acknowledgments

The research leading to these results has been carried out under the framework of the project "FuturePorts". The project started in January 2022 and is led by the Program Directorate Transport within the German Aerospace Center (DLR), whose support we greatly appreciate.

References

[1] Faber Jasper, Hanayama Shinichi, Zhang Shuang, Pereda Paula, Comer Bryan, Hauerhof Elena et al. Fourth IMO greenhouse gas study 2020: Full report. London, UK: International Maritime Organization; 2021.
[2] Xing Hui, Stuart Charles, Spence Stephen, Chen Hua. Alternative fuel options for low carbon maritime transportation: Pathways to 2050. J Clean Prod 2021;297:126651. http://dx.doi.org/10.1016/j.jclepro.2021.126651.
[3] Alvestad Lars, Berge Kolbjørn. Handbook for hydrogen-fuelled vessels: MarHySafe JDP phase 1. 1st ed.. Maritime Hydrogen Safety (MarHySafe) Joint Development Project and DNV; 2021.
[4] Rivard Etienne, Trudeau Michel, Zaghib Karim. Hydrogen storage for mobility: A review. Materials 2019;12(12). http://dx.doi.org/10.3390/ma12121973.
[5] Klebanoff LE, Pratt JW, LaFleur CB. Comparison of the safety-related physical and combustion properties of liquid hydrogen and liquid natural gas in the context of the SF-breeze high-speed fuel-cell ferry. Int J Hydrog Energy 2017;42(1):757–74. http://dx.doi.org/10.1016/j.ijhydene.2016.11.024, URL https://www.sciencedirect.com/science/article/pii/S036031991633316X.

[6] Duong Phan Anh, Ryu Bo Rim, Jung Jinwon, Kang Hokeun. A comprehensive review of the establishment of safety zones and quantitative risk analysis during ship-to-ship LNG bunkering. Energies 2024;17(2):512. http://dx.doi.org/10.3390/en17020512.

[7] Saborit Enrique, García-Rosales Vazquez Eduardo, Storch de Gracia Calvo M Dolores, Rodado Nieto Gema María, Martínez Fondón Pablo, Abánades Alberto. Alternatives for transport, storage in port and bunkering systems for offshore energy to green hydrogen. Energies 2023;16(22). http://dx.doi.org/10.3390/en16227467, URL https://www.mdpi.com/1996-1073/16/22/7467.

[8] Duong Phan Anh, Ryu Bo Rim, Jung Jinwon, Kang Hokeun. Comparative analysis on vapor cloud dispersion between LNG/liquid NH3 leakage on the ship to ship bunkering for establishing safety zones. J Loss Prev Process Ind 2023;85:105167. http://dx.doi.org/10.1016/j.jlp.2023.105167.

[9] Fan Hongjun, Enshaei Hossein, Gamini Jayasinghe Shantha. Safety philosophy and risk analysis methodology for LNG bunkering simultaneous operations (SIMOPs): A literature review. Saf Sci 2021;136:105150. http://dx.doi.org/10.1016/j.ssci.2020.105150.

[10] Braglia Marcello, Frosolini Marco, Montanari Roberto. Fuzzy criticality assessment model for failure modes and effects analysis. Int J Qual Reliab Manag 2003;20(4):503–24. http://dx.doi.org/10.1108/02656710310468687.

[11] Risktec TÜV Rheinland. Quantitative Risk Assessment (QRA): An introduction to the quantitative assessment of risks associated with high hazard facilities. TÜV Rheinland Risktec; 2018, URL https://www.risktec.tuv.com/wp-content/uploads/2018/11/Risktec-QRA-brochure-i1.0-med-res-single-pages.pdf.

[12] Tofalos Charalampos, Jeong Byongug, Jang Hayoung. Safety comparison analysis between LNG/LH_2 for bunkering operation. J Int Marit Saf Environ Aff Shipp 2020;4(4):135–50. http://dx.doi.org/10.1080/25725084.2020.1840859.

[13] Jeong Byongug, Lee Byung Suk, Zhou Peilin, Ha Seung-man. Evaluation of safety exclusion zone for LNG bunkering station on LNG-fuelled ships. J Mar Eng Technol 2017;16(3):121–44. http://dx.doi.org/10.1080/20464177.2017.1295786.

[14] Kopp Martin. Kreuzfahrt: Diese Schiffe starten 2023 im Hamburger Hafen. Hamburger Abendblatt 2023;2023. URL https://www.abendblatt.de/wirtschaft/article238040853/Hamburg-erwartet-so-viele-Schiffe-wie-nie.html.

[15] Jeong Byongug. On the safety of LNG-fuelled ships (Ph.D. thesis), Glasgow: Department of Naval Architecture, Ocean and Marine Engineering; June 2018, URL https://stax.strath.ac.uk/concern/theses/pg15bd88s.

[16] International Association of Oil & Gas Producers. Process release frequencies: Risk assessment data directory. Report 434-01, 2019.

[17] DNVDet Norske Veritas. Failure frequency guidance: process equipment leak frequency data for use in QRA. 2013.

[18] Cox AW, Lees FP, Ang ML. Classification of hazardous locations. London: Institution of Chemical Engineers; 1990.

[19] National Institute of Public Health and the Environment (RIVM) Centre for External Safety. Reference manual bevi risk assessments. 2009, URL https://www.rivm.nl/sites/default/files/2018-11/Reference-Manual-Bevi-Risk-Assessments-version-3-2.pdf.

[20] International Association of Oil & Gas Producers. Ignition Probabilities: Risk Assessment Data Directory. 2019.

[21] Woodward John Lowell. LNG risk based safety: Modeling and consequence analysis. Hoboken, N.J and New York: Wiley and AIChE; 2010, http://dx.doi.org/10.1002/9780470590232, URL https://onlinelibrary.wiley.com/doi/book/10.1002/9780470590232.

[22] Verfondern K, Dienhart B. Pool spreading and vaporization of liquid hydrogen. Int J Hydrog Energy 2007;32(2):256–67. http://dx.doi.org/10.1016/j.ijhydene.2006.01.016.

[23] Raj Phani K. LNG fires: a review of experimental results, models and hazard prediction challenges. J Hazard Mater 2007;140(3):444–64. http://dx.doi.org/10.1016/j.jhazmat.2006.10.029.

[24] Weiner Ruth F, Matthews Robin A. Environmental engineering, 4th ed., updated ed.. Amsterdam: Butterworth-Heinemann; 2003, URL http://www.loc.gov/catdir/description/els031/2003050203.html.

[25] Lobato Justo, Rodríguez Juan F, Jiménez Carlos, Llanos Javier, Nieto-Márquez Antonio, Inarejos Antonio M. Consequence analysis of an explosion by simple models: Texas refinery gasoline explosion case. Afinidad J Chem Eng Theor Appl Chemist 2009;2009(Vol. 66). URL https://raco.cat/index.php/afinidad/article/view/279547.

[26] IMOInternational Maritime Organization. Revised guidelines for formal safety assessment (Fsa) for use in the IMO rule-making process: MSC-MEPC.2/Circ.12/Rev.2. 2018, URL https://wwwcdn.imo.org/localresources/en/OurWork/HumanElement/Documents/MSC-MEPC.2-Circ.12-Rev.2%20-%20Revised%20Guidelines%20For%20Formal%20Safety%20Assessment%20(Fsa)For%20Use%20In%20The%20Imo%20Rule-Making%20Proces...%20(Secretariat).pdf.

[27] International Association of Oil & Gas Producers. Vulnerability of humans: Risk assessment data directory. Report 434-14, 2023.

[28] Hyresponder. Properties of hydrogen relevant to safety: Lecture 2. level IV specialist officer. 2021, URL https://hyresponder.eu/e-platform/training-materials/educational-training/lecture-2-properties-of-hydrogen-relevant-to-safety/.